First European Conference on Earthquake Engineering and Seismology
(a joint event of the 13th ECEE & 30th General Assembly of the ESC)
Geneva, Switzerland, 3-8 September 2006
Paper Number: 1171

AGGRAVATION OF SEISMIC GROUND MOTION DUE TO SLOPE TOPOGRAPHY

George BOUCKOVALAS[1] and Achilleas PAPADIMITRIOU[2]

SUMMARY

This paper presents results from parametric numerical analyses for the seismic response of step-like ground slopes, under vertically propagating SV waves. The analyses explore the effects of slope geometry, dynamic soil properties, predominant frequency and duration of the excitation on the aggravation of the seismic ground motion. The results show intense geographic variability of horizontal motion, with a general trend of amplification near the crest and de-amplification near the toe of the slope. In addition, this study highlights a parasitic vertical component of motion in the vicinity of the slope, that is generated by wave reflections at the slope surface and that under certain preconditions may become as large as the horizontal component. Hence, reliable field evidence of topographic aggravation of seismic ground motion requires extremely dense arrays. From an engineering point of view, criteria are established for deciding on the importance of topography effects, while approximate relations are provided for the preliminary evaluation of the topographic aggravation of seismic ground motion and the width of the affected zone behind the crest. The reliability of the foregoing criteria and approximate relations is verified against results from case studies and existing code provisions.

1. INTRODUCTION

The effect of step-like slope topography on seismic ground motion has not been thoroughly examined in the literature, despite that there is indisputable evidence of its significance even from the late 1960's. Among the published studies, the majority concerns either specific geometries and seismic excitations [e.g. Bouckovalas et al, 1999; Athanasopoulos et al, 2001; Gazetas et al, 2002; Assimaki and Gazetas, 2004], or examines specific aspects of the phenomenon such as the wave scattering generated at the vicinity of the slope [Boore et al, 1981] and the effects of a soft soil cap in the area of the slope [Ohtsuki and Harumi, 1983]. The only systematic parametric study found in the literature is that by Ashford and Sitar (1997) and Ashford et al (1997), which provides valuable insight to the effects of slope inclination i and height H, wave type (P, SH and SV) and wavelength λ, as well as the angle of wave incidence β. Nevertheless, the results of the analyses are presented solely at the crest and at distances equal to H, $2H$ and $4H$ behind it. Furthermore, these parametric studies do not address the effect of two (2) factors that are commonly accounted for in most seismic ground response analyses: the hysteretic damping ratio of the soil ξ and the duration of the shaking or the number of equivalent uniform excitation cycles N. Thus, the results presented in these studies cannot be readily used for a quantitative assessment of the effect of slope topography on seismic ground motion, in the form of either simple approximate relations or seismic code provisions.

Aiming at this goal, results are presented from an extensive parametric study of step-like slope topography effects, performed with FLAC (Itasca Inc, 1993). The relevant research was triggered from recent evidence that such effects played an important role in the extent of damage caused by two (2) recent destructive earthquakes in

[1] Professor, Geotechnical Dept., School of Civil Engineering, National Technical University of Athens, 15780, Zografou, Greece
Email : gbouck@central.ntua.gr
[2] Research Fellow, Geotechnical Dept., School of Civil Engineering, National Technical University of Athens, 15780, Zografou, Greece
Email: loupapas@alum.mit.edu

Greece: the 1995 Aigion event [Bouckovalas et al, 1999] and the 1999 Athens event [Athanasopoulos et al, 2001; Gazetas et al, 2002]. Compared to the studies by Ashford and Sitar (1997) and Ashford et al (1997), our study is narrower in the sense that it focuses merely on the case of vertically propagating SV waves. On the other hand, it explores in detail the effects of a larger number of problem parameters and provides a continuous assessment of topography aggravation all along the ground surface, both behind the crest and in front of the toe of the step-like slope. It should be underlined, that the quantitative assessments hereby provided apply conservatively to SH waves as well, since SH topographic aggravation has been shown smaller than that of SV waves [Ashford and Sitar, 1997; Ashford et al, 1997]. Note that details on the hereby presented numerical results can be found in Bouckovalas and Papadimitriou (2005). This paper adds to the latter work in terms of the topographic aggravation envelope of spatial variation and the proposal for a tentative set of code provisions.

2. OUTLINE OF METHODOLOGY

The numerical analyses were performed with the FLAC [Itasca, 1993], for linear visco-elastic soil with V_S = 500m/s, Poisson's ratio v = 1/3 and mass density ρ = 2Mg/m^3. A schematic illustration of the 2D analyzed mesh and the boundary conditions is provided in Fig. 1. More specifically,

- 28000 to 120000 quadrilateral zones were used to simulate the uniform soil mass, with a maximum height equal to 1/10 – 1/20 of the predominant wavelength of the seismic excitation in order to avoid the numerical distortion of its frequency content.
- The width and the height of the mesh were usually set at *20H* and *5H* respectively, in order to reduce the effects of artificial wave reflections from the boundaries at the area of interest (near the slope).
- For the same purpose, transmitting boundaries were applied at the base of the mesh, while boundaries simulating the free field were applied at its right and left sides.
- Unlike common practice that introduces the seismic excitation at the base of the mesh as a time history of acceleration (or velocity, or displacement), in our analyses a time history of shear stress was used, in order to avoid artificial wave reflections at the base of the mesh, which are unavoidable in analyses of common practice.
- Most of the parametric analyses were performed either with a harmonic excitation of 20 – 40 uniform cycles, or with a Chang's Signal excitation aimed to simulate the limited duration as well as the gradual rise and decrease of shaking amplitude (Fig. 1). In addition, a limited number of parametric analyses were performed for actual seismic excitations to explore the effect of a much wider frequency content.

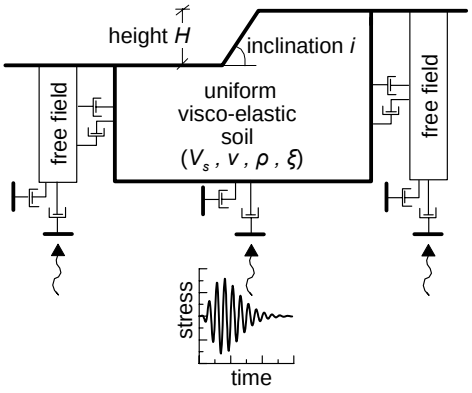

Figure 1: Schematic illustration of the 2D mesh and the boundary conditions

It is important to notice that the accuracy of the previously outlined numerical methodology was verified through comparisons to analytical solutions for topographies of various forms in uniform elastic half-space [Bouckovalas and Papadimitriou, 2005]. In addition, note that the results of the numerical analyses are not evaluated directly, but following normalization against the free-field response of the ground, which is free from any topography effects. For this purpose, each reference 2D analysis was supplemented by two 1D analyses: one for the free field in front of the toe of the slope and the other for the free field behind its crest. This approach is cumbersome, but more accurate than evaluating the free-field response from the results of the 2D analyses alone, at nodes at large distance away from the slope. The reason is that topography effects decrease asymptotically with distance from the slope and may not completely disappear within the analyzed mesh, thus underestimating the overall amplification effects, especially for low intensity motions with small soil damping.

3. TYPICAL RESULTS

Typical results from the numerical analyses are presented in Fig. 2, for the specific case of uniform soil, slope inclination $i = 30^o$, normalized height $H/\lambda = 2.0$, critical damping ratio $\xi = 5\%$ and six significant cycles of base excitation ($N = 6$). This figure shows the variation of the topography aggravation factors $A_h=a_h/a_{h,ff}$ and $A_v=a_v/a_{h,ff}$ with distance from the crest x, where a_h and a_v denote the peak horizontal and peak vertical accelerations at each point of the ground surface.

Parameter $a_{h,ff}$ denotes the free-field value for the peak horizontal acceleration and is used for normalization of both a_h and a_v, since $a_{v,ff} = 0$ for a vertically propagating SV wave in a uniform horizontal soil. Review and interpretation of this figure alone provides insight to the mechanisms, which control topography aggravation and lead to some first conclusions of practical interest. Namely:

(a) Even a purely horizontal excitation, as a vertically propagating SV wave, results in considerable (parasitic) vertical motion at the ground surface near the slope. As shown in this figure, this parasitic vertical motion may be of comparable intensity to that of the horizontal free-field motion, under certain preconditions of soil, topography and excitation conditions.

(b) The topography aggravation of the horizontal ground motion, expressed through the acceleration ratio $A_h=a_h/a_{h,ff}$, fluctuates intensely with distance away from the crest of the slope, alternating between amplification ($A_h > 1.0$) and de-amplification ($A_h < 1.0$) within very short horizontal lengths. Similarly, the parasitic vertical motion expressed via A_v is also intensely variable with distance. In particular, the distance between local maxima and minima is shown to be approximately equal to λ for both the horizontal and the vertical motion. Yet, as a general trend, the horizontal ground motion is de-amplified at the toe of the slope and amplified near the crest.

(c) The above findings can be readily attributed to the reflection of the incoming SV waves on the inclined free surface of the slope, which leads to reflected P and SV waves impinging obliquely at the free ground surface behind the crest, as well as Rayleigh waves traveling along the surface behind the crest and before the toe. All these induced waves have a strong vertical component. In addition, they arrive with a time lag and a phase difference at the different points of the ground surface so that their superposition to the incoming SV waves may lead either to amplification or to de-amplification of the horizontal seismic motion.

(d) Hence it may be argued that the intense fluctuation of topographic aggravation implies that its experimental verification through inverse analysis of structural damage is very crude, and that actual ground motion recordings near slopes must be obtained via very dense seismic arrays.

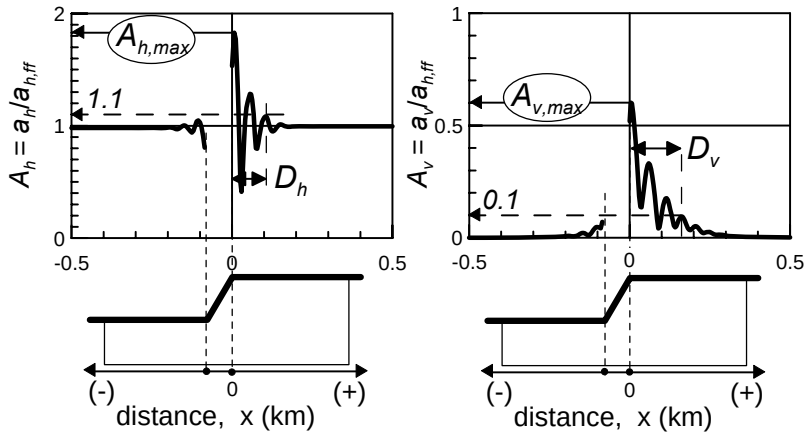

Figure 2: Typical results for the topographic aggravation of the peak horizontal A_h and the peak parasitic vertical A_v acceleration, as a function of horizontal distance x from the crest (for H/λ=2, i=30^o, N=6, ξ=5%)

4. APPROXIMATE RELATIONS

In all, 90 parametric analyses were performed in order to assess the effect of the following important parameters:

- the slope inclination $i(^o)$ or $I=i/90$, with a variation of $i = 10^o – 90^o$ ($I = 0.11 – 1.0$),
- the normalized height of the slope H/λ, with a variation of $H/\lambda = 0.05 – 2.0$,
- the number of significant excitation cycles N, i.e. those whose intensity exceeds 50% of the peak, with a variation of $N = 1 – 12$,
- the critical hysteretic damping ratio ξ of the soil, with a variation of $\xi = 0 – 20\%$.

Note that the 90 parametric analyses were performed for base excitations with a predominant period T_e ranging from 0.05 – 2.0sec, a range practically covering the large majority of possible earthquake events. This range of T_e is what produces the foregoing range of H/λ = 0.05 – 2.0 since all analyses were performed for a slope of height H = 50m and uniform V_s = 500m/s. Nevertheless, topographic aggravation results coincide for step-like slopes with different values of H and λ but the same value of H/λ, a fact that allows for the generalization of the presented results for a very large range of soil and excitation conditions [Ashford et al, 1997].

Figures 3 and 4 present indicative results from the parametric analyses demonstrating the effects of slope angle i and normalized height H/λ. It is observed that these two (2) parameters have a significant and non-univocal effect on the aggravation of the horizontal and vertical ground motions (factors A_h and A_v, respectively), as well as on the distance to the free field in front and behind the slope. On the contrary, soil damping ξ has an important (reducing) effect merely on the distance to the free field, while the number of significant cycles N was found of small importance [Bouckovalas and Papadimitriou, 2005]. Practically speaking, our results in terms of A_h and A_v from analyses for small soil damping ($\xi \leq 5\%$) agree in both qualitative and quantitative terms with the works of Ashford and Sitar (1997) and Ashford et al (1997).

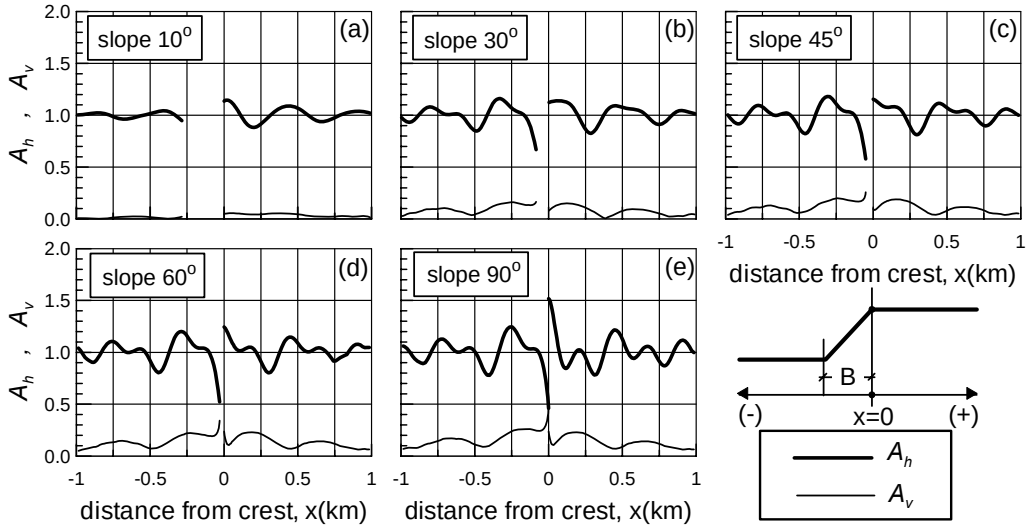

Figure 3: Effect of slope inclination *i* on the aggravation of the peak horizontal A_h and the peak parasitic vertical A_v acceleration, as a function of horizontal distance x from the crest of a step-like slope (for H/λ = 0.2, harmonic motion, ξ < 5%)

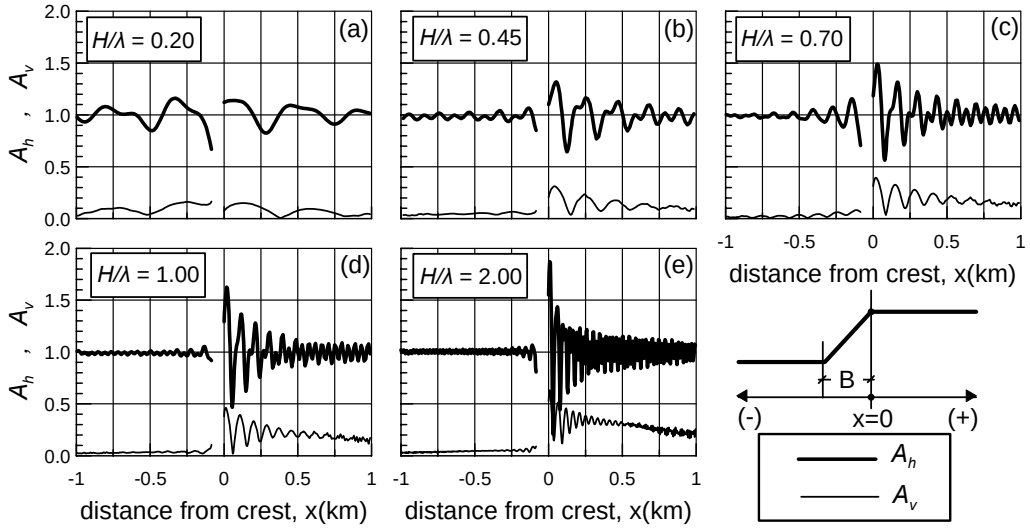

Figure 4: Effect of normalized height H/λ on the aggravation of the peak horizontal A_h and the peak parasitic vertical A_v acceleration, as a function of horizontal distance x from the crest of a step-like slope (for i=30°, harmonic motion, ξ < 5%)

In order to increase the applicability of the results of the parametric analyses, a database was created tabulating the most important input variables and output parameters of all ninety (90) analyses. Namely, the input of each analysis was introduced in terms of variables *I(=i/90), H/λ, N* and *ξ*. The selection of the output parameters was less straightforward. Addressing this issue from an engineering point of view, of interest for design purposes of civil engineering works are (see Fig. 2):

- the peak values of the topography aggravation factors $A_{h,max}$ and $A_{v,max}$ behind the crest, in the horizontal and vertical direction, respectively, and
- the distances D_h and D_v behind the crest at which the seismic ground motion is not affected by the existence of the slope (free field conditions), defined as the minimum distances where $A_h \leq 1.10$ and $A_v \leq 0.10$.

These four (4) design parameters were related statistically (via an iterative Newton-Raphson procedure) to the four (4) input variables via the following general expressions [Bouckovalas and Papadimitriou, 2005]:

$$A_{h,max} = 1 + \frac{0.225\left(H/\lambda\right)^{0.4}\left(\frac{I^2+2I^6}{I^3+0.02}\right)}{1+0.9\xi} \tag{1}$$

$$A_{v,max} = \frac{0.75\left(H/\lambda\right)^{0.8}\left(I^{0.5}+1.5I^5\right)}{1+0.15\xi^{0.5}} \tag{2}$$

$$D_h/H = \frac{\left[\frac{\left(H/\lambda\right)}{0.2+\left(H/\lambda\right)^2}\right]\left(\frac{I^{1.5}+3.3I^8}{I^4+0.07}\right)}{0.71+3.33\xi} N^{0.43} \tag{3}$$

$$D_v/H = \frac{\left[\frac{0.233\left(H/\lambda\right)}{0.2+\left(H/\lambda\right)^2}\right]\left(\frac{I^{1.5}+3.3I^8}{I^4+0.07}\right)}{\xi^{0.78}} \tag{4}$$

The comparison between approximate and numerical predictions of $A_{h,max}$, $A_{v,max}$, D_h/H and D_v/H for all ninety (90) analyses is shown in the four plots of Figure 5. The diagonal lines in each plot correspond to perfect match between the compared values, while the shaded area provides an estimate of the anticipated relative difference. Observe that, the symbols are equally scattered on both sides of the diagonal lines and that the standard deviation of the relative error of the approximate relations ranges from 29 to 40%, depending on the parameter at hand.

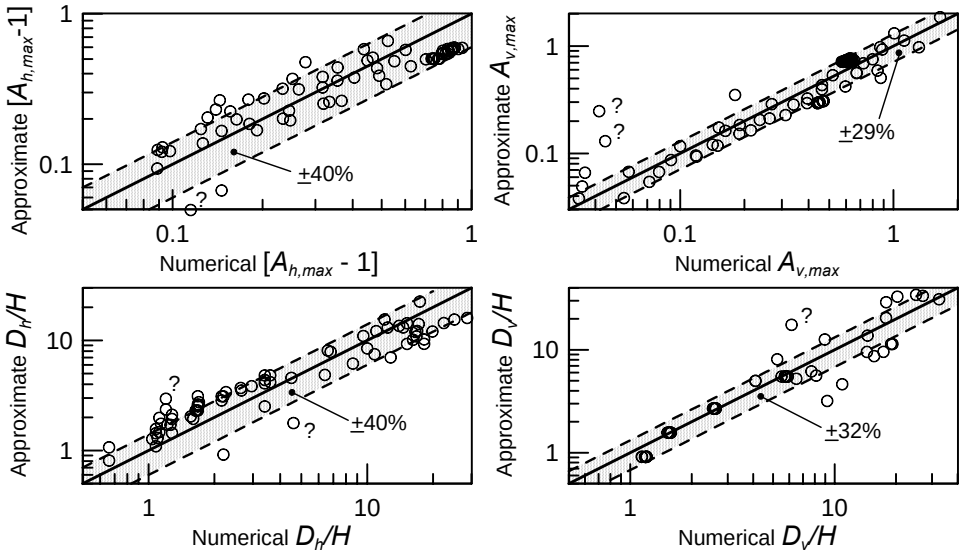

Figure 5: Comparison of $A_{h,max}$, $A_{v,max}$, D_h/H and D_v/H estimates from approximate relations and numerical analyses for all the cases in the database

Eqs 1 through 4 may be considered analytically complicated and not insightful from an engineering point of view. While we agree that this is true, their functional depicts the fact that the effects of H/λ and I are not univocal. The obvious alternative would be to introduce multi-partite simple relations, i.e. different simple relations for different ranges of H/λ and I for each of the four (4) design parameters. This was not opted because it would lead to a set of relations for each of the four (4) parameters, which is considered as an overall more complicated solution than a single relation for each parameter.

The topographic aggravation of the seismic motion in the horizontal and vertical directions as a function of $A_{h,max}$ and $A_{v,max}$ for the whole distance D_h and D_v behind the crest is considered extremely conservative and non compliant to the results of the analyses. Hence, the results of the variation of A_h and A_v with distance x from the crest of the slope for each one of the ninety (90) analyses were normalized to the respective values of $A_{h,max}$, $A_{v,max}$, D_h and D_v and plotted together in Figure 6.

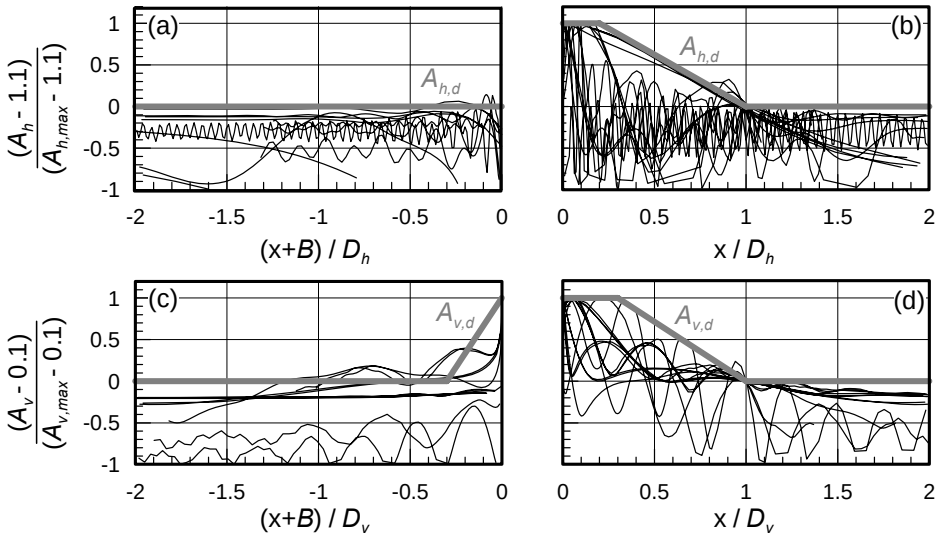

Figure 6: Design envelopes $A_{h,d}$ and $A_{v,d}$ of the topography aggravation factors A_h and A_v with distance x from the crest of the slope ($B = H/\tan i$)

Based on this figure, design envelopes were defined, denoted as $A_{h,d}$ and $A_{v,d}$, for the geographic variation of A_h and A_v with distance x from the crest of the slope. These design envelopes are given by Eqs. (5) and (6) below:

$$A_{h,d} = \begin{cases} 1.0 \div 1.1 & , \quad x \le -B \\ 1.1 + \dfrac{A_{h,max} - 1.1}{B}(x + B) & , \quad -B \le x \le 0 \\ A_{h,max} & , \quad 0 \le x \le 0.2D_h \\ A_{h,max} - \dfrac{A_{h,max} - 1.1}{0.8D_h}(x - 0.2D_h) & , \quad 0.2D_h \le x \le D_h \\ 1.0 \div 1.1 & , \quad D_h \le x \end{cases} \tag{5}$$

$$A_{v,d} = \begin{cases} 0.0 \div 0.1 & , \quad x \le -(B + 0.3D_v) \\ 0.1 + \dfrac{A_{v,max} - 0.1}{0.3D_v}(x + B + 0.3D_v) & , \quad -(B + 0.3D_v) \le x \le -B \\ A_{v,max} & , \quad -B \le x \le 0.3D_v \\ A_{v,max} - \dfrac{A_{v,max} - 0.1}{0.7D_v}(x - 0.3D_v) & , \quad 0.3D_v \le x \le D_v \\ 0.0 \div 0.1 & , \quad D_v \le x \end{cases} \tag{6}$$

5. COMPARISON WITH CODE PROVISIONS

The comparison of the foregoing results with code provisions leads to useful conclusions regarding the compatibility between the codes and the theory-based simulations. Extensive search in the literature showed that only EC-8 (2000 and draft of 2002) and the French Seismic Code PS-92 have provisions related to the topographic aggravation of seismic motion. In particular, for the topography of a slope the two codes prescribe an increase of the peak horizontal acceleration by 20% and 40%, respectively, while they both disregard the apparition of parasitic vertical motion. In EC-8, the increase of the horizontal acceleration is prescribed for areas "*near the top edge*", i.e. the distance to the free field is relatively small but not clearly defined. On the contrary, the PS-92 code provides specific relations for the estimation of this distance, according to which this distance rarely exceeds the height H of the slope. In addition, the two codes prescribe lower bounds for the geometric dimensions of the slope, below which topographic aggravation of seismic ground motion should be ignored. Namely, the EC-8 prescribes topographic aggravation only if the slope height $H > 30$m and the slope inclination $i > 15^o$, while the PS-92 adopts the following bounds: $H > 10$m and $i > 22^o$.

To perform a comparison of the foregoing code provisions with the results of our analyses, the latter should be processed in order to establish the average values of $A_{h,max}$, $A_{v,max}$ and the distance D to the free field behind the crest (i.e. of the maximum of the D_h and D_v) for common cases of practical interest. Similarly, criteria for the relative significance of the topographic aggravation should be prescribed on the basis of the results of our analyses.

In most cases, the input parameters of the relations take the following values: $H/\lambda = 0.2 \div 1.0$, $i = 25 \div 75^o$ and $\xi = 5 \div 15\%$. These values lead to a usual range of $A_{h,max} = 1.20 \div 1.50$ and $A_{v,max} = 0.20 \div 1.10$, while the distance D ranges from $2H$ to $8H$. Hence, the code provisions are compatible with the theoretical predictions in terms of the amplification of the peak horizontal acceleration, but clearly underestimate the distance to the free field. In addition, the fact that the parasitic vertical motion is found relatively significant in common cases of practice, shows a problem of the existing code provisions. In order to establish criteria for the relative importance of topographic aggravation, Figure 7 presents the pairs of values for the most important parameters H/λ and $I=i/90^o$ for which the values of $A_{h,max} \geq 1.10$ & 1.20 and $A_{v,max} \geq 0.10$ & 0.20. The value of damping ξ in Figure 7 has a small effect on the results, and was assumed equal to 10%, a value characteristic of strong earthquake motion. From Figure 7 it is concluded that the criteria for significant topographic aggravation of the horizontal acceleration (i.e. $A_{h,max} \geq 1.10$ & 1.20) are more strict than those for the apparition of significant parasitic vertical motion (i.e. $A_{v,max} \geq 0.10$ & 0.20). Hence, adopting the former

– $H/\lambda > 0.03$ and $i > 10^o$ for at least 10% topographic aggravation of the horizontal motion, and
– $H/\lambda > 0.16$ and $i > 17^o$ for at least 20% topographic aggravation of the horizontal motion.

The foregoing criteria are considered more rational than the purely geometrical criteria of the code provisions, since they include the predominant wavelength λ, which takes into account (in an approximate manner) the local soil conditions and a crucial characteristic of the seismic excitation. Yet, for usual cases of slopes that have $V_s > 400$m/s (stiff soils or soft rocks) and for common seismic excitations with a predominant period larger than 0.20s, the code provisions for lower bounds are in broad agreement with the hereby proposed criteria for 20% topographic aggravation that lead to $H > 13$m and $i > 17^o$.

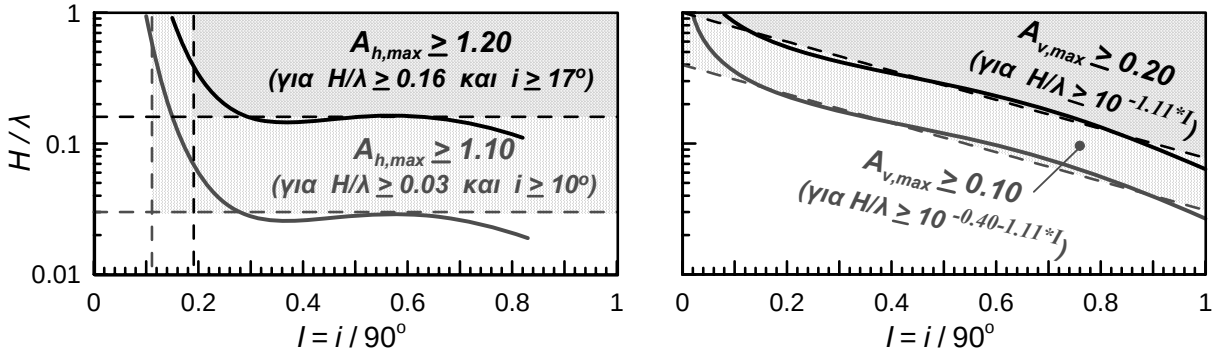

Figure 7: Lower limits of normalized slope height H/λ and slope angle i, for which topography effects become significant.

6. COMPARISON WITH CASE STUDIES

The excitations used to perform the parametric analyses were harmonic or nearly harmonic (Chang signal), with a very narrow frequency spectrum as compared to seismic recordings. To explore the importance of this limitation, the proposed relations have been applied to predict the results of three (3) numerical case studies for seismic events in Greece, namely:

a) the slope in Aigion city with an inclination $i \cong 45^o$, height $H \cong 80$m in the Aigion earthquake, 15-6-95, [Bouckovalas et al, 1999].
b) the slope of the Kifissos river in Adames with an inclination $i \cong 30^o$, height $H \cong 40$m in the Athens earthquake, 7-9-99, [Gazetas et al, 2002].
c) the slope of the Kifissos river at the site of hotel "Dekelia" with an inclination $i \cong 16^o$, height $H \cong 35$m in the Athens earthquake, 7-9-99, [Athanasopoulos et al, 2001].

Unfortunately, in all three (3) cases there were no concurrent seismic recordings at the slope and at the free field. Therefore, the case-specific analyses had a parametric nature and the topographic aggravation, in terms of $A_{h,max}$ and D_h, was estimated as a range of possible variation by the aforementioned researchers. Similarly, the estimates from the proposed relations lead to ranges of possible variation. Hence, the comparison of the estimates from the analyses and the relations is depicted by the rectangles of Figure 8, from which a satisfactory agreement is observed. Details on these comparisons are presented by Bouckovalas and Papadimitriou (2005).

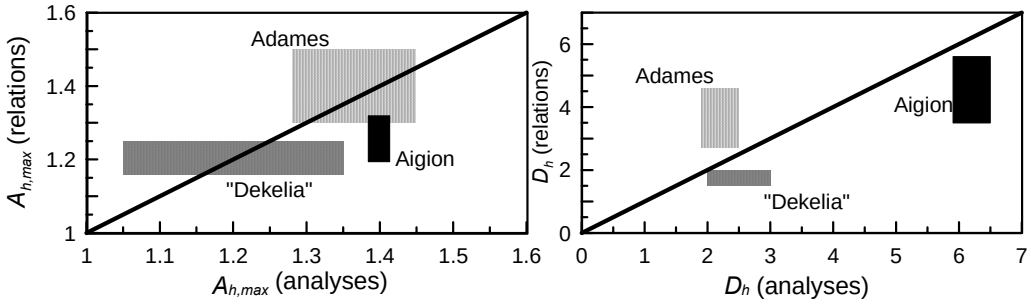

Figure 8: Comparison of topographic aggravation predictions in terms of $A_{h,max}$ and D_h for case histories, as resulting from detailed numerical analyses and the proposed relations .

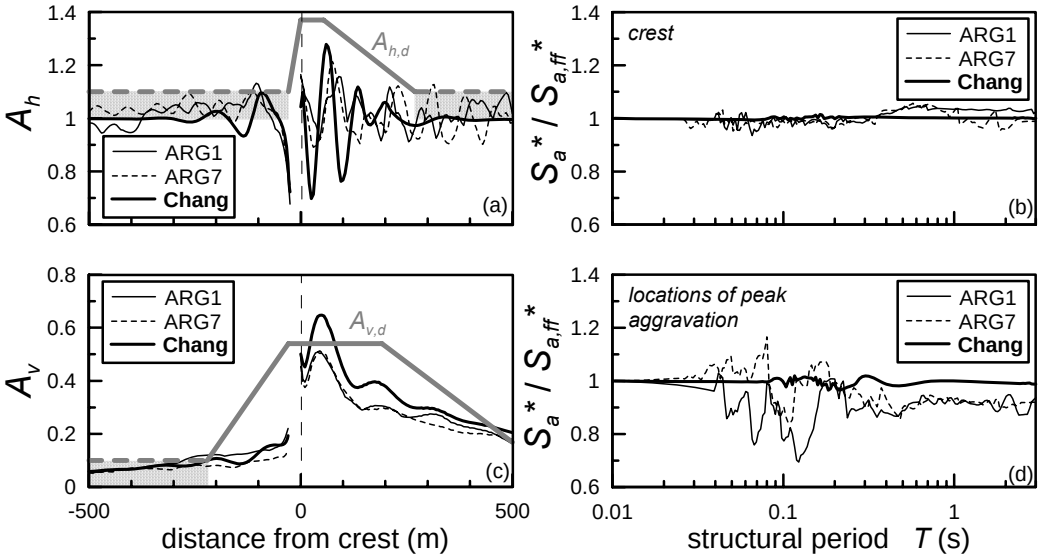

Figure 9: Comparison of topographic aggravation from the proposed approximate relations and numerical analyses with seismic recordings (ARG1 and ARG7) and an equivalent Chang signal.

In addition, a numerical "experiment" was performed, i.e. a slope with $H = 50$m, $i = 60^o$ consisting of a linear visco-elastic soil with $V_s = 500$m/s, Poisson's ratio $\nu = 1/3$ and mass density $\rho = 2$Mg/m^3 was subjected to three (3) base excitations, two recordings (ARG1 and ARG7) with similar values of $T_e = 0.14 - 0.16$s and $N = 2 - 4.5$ and a Chang signal with similar characteristics. Figures 9a and 9b compare the variations of A_h and A_v with

distance x from the crest resulting from the three (3) numerical analyses to the respective aggravation envelopes $A_{h,d}$ and $A_{v,d}$ from Equations (1) to (6). The results from the three (3) analyses compare well with one another, with the Chang signal analysis being rather conservative. In addition, the results from all three (3) analyses generally fall below the proposed design envelope, with the exception of a small under-prediction of the $A_{v,max}$ but only in the Chang signal analysis. Furthermore, Figures 9c & 9d present the topographic aggravation of the normalized elastic response spectrum (5% damping) $S_a^* = S_a/a_h$ at two locations: a) the crest and b) the point of peak aggravation (where $A_h = A_{h,max}$), disregarding the fact that the locations of peak aggravation in the three analyses are neighborly, but do not coincide. These results show that topography seems to affect mostly the peak ground acceleration and less so its frequency content.

7. TENTATIVE PROPOSAL FOR CODE PROVISIONS

Under the understanding that our results have been based merely on numerical analyses and still require further experimental verification, we come to propose a tentative set of code provisions for topography aggravation, by simplifying further the proposed relations and criteria. In particular, the proposed provisions built on the current state of the (Informative) Annex A of EC-8 pertaining to topographic amplification factors (paragraphs A.1, A.2 and A.3) and are presented here more as a basis of discussion, rather than a concrete set of ready-to-be-implemented code provisions. Hence, the following modifications to code provisions of EC-8 are proposed, for the cases of *slopes* (a 2D topographic irregularity):

(a) Topography aggravation may be neglected, if the average *slope* inclination $i < 17^o$ and the height of the *slope* $H < \max[13\text{m}, 0.16\lambda]$, where λ is the predominant wavelength of the shear waves in the *slope*. Otherwise, explicit use of frequency-independent topography aggravation factors should be used for the design of important structures ($\gamma_I > 1.0$) in the vicinity of *slopes*.

(b) In general, two (2) topography aggravation factors are defined, one for the horizontal and one for the vertical direction, that are denoted as S_{hT} and S_{vT}, respectively. These factors scale the ordinates of the horizontal elastic design response spectrum given in EN 1998-1:2004 and lead to amplified horizontal seismic actions and additional vertical seismic actions, that should be superimposed to those resulting from the vertical elastic response spectrum given in EN 1998-1:2004.

(d)For *slopes* that are both higher and steeper than the above lower bounds, the topographic amplification factors vary with location. If x is the horizontal distance from the crest of the slope (where x > 0 behind the crest), the amplification factors per location x are given by:

$$S_{hT} = \left\{ \begin{array}{lll} 1.1 + \dfrac{A_{h,max} - 1.1}{B}(x + B) & , & x \le 0 \\ A_{h,max} & , & 0 \le x \le 0.2D \\ A_{h,max} - \dfrac{A_{h,max} - 1.1}{0.8D}(x - 0.2D) & , & 0.2D \le x \end{array} \right\} \ge 1.0 \tag{7}$$

$$S_{vT} = \left\{ \begin{array}{lll} 0.1 + \dfrac{A_{v,max} - 0.1}{0.2D}(x + B + 0.2D) & , & x \le -B \\ A_{v,max} & , & -B \le x \le 0.2D \\ A_{v,max} - \dfrac{A_{v,max} - 0.1}{0.5D}(x - 0.2D) & , & 0.2D \le x \end{array} \right\} \ge 0.0 \tag{8}$$

where $B = H/\tan i$, the horizontal projection of the slope, $A_{h,max}$ and $A_{v,max}$ the coefficients of maximum topographic aggravation for the horizontal and parasitic vertical motions and *D is* the distances to the free field behind the crest, that are given in simplified form by:

$$A_{h,max} = 0.2(H/\lambda)^{0.4}\left(\frac{I^2 + 2I^6}{I^3 + 0.02}\right) \tag{9}$$

$$A_{v,max} = 0.7(H/\lambda)^{0.8}\left(I^{0.5} + 1.5I^5\right) \tag{10}$$

$$D/H = 2\left[\frac{(H/\lambda)}{(\mathrm{H}/\lambda)^2 + 0.2}\right]\left(\frac{\mathrm{I}^{1.5} + 3.3\mathrm{I}^8}{\mathrm{I}^4 + 0.07}\right) \tag{11}$$

where $I = \mathrm{i}/90^{\mathrm{o}}$. Note that Equations 7, 8 and 11 imply that $D = D_h$ and $D_v = 0.7D_h$ for most cases in practice.

8. CONCLUSIONS

The basic conclusions from this study are the following:

(a) Slope topography alters (increases and decreases) mainly the peak acceleration and less so the frequency content of the horizontal seismic motion. In addition, it creates a parasitic vertical motion. These effects are pronounced in the vicinity of the slope and decrease with distance.

(b) Amplification of the horizontal motion is generally expected behind the crest of the slope, while the opposite effect (i.e. de-amplification) is generally expected in front of the toe of the slope. Despite the foregoing trends, intense geographic variability of the (horizontal and vertical) seismic motion is expected, even within tens of meters. Hence, the detection of topography aggravation effects on the basis of field recordings can only be achieved with very dense arrays.

(c) This paper presents approximate relations for the estimation of the coefficients of topographic aggravation of the peak horizontal and vertical acceleration $A_{h,max}$ and $A_{v,max}$, as well as their relative distances to the free field, D_h and D_v. In addition, a geographic design envelope of topographic aggravation is proposed for the horizontal and vertical motion, $A_{h,d}$ and $A_{v,d}$. Overall, the proposed approximate relations are in satisfactory agreement with case-specific numerical analyses.

(d) Topography aggravation is considered significant only when $H/\lambda > 0.16$ and the slope inclination $i > 17^{\mathrm{o}}$. In such cases, the values of the coefficients of maximum topographic aggravation for the horizontal and vertical seismic motion range from $A_{h,max} = 1.20 - 1.50$ and $A_{v,max} = 0.20 - 1.10$, while the distance to the free field ranges from $D = 2H - 8H$.

(e) The only Seismic Codes that deal with topographic aggravation (EC-8 and PS-92) give rational values for the amplification of the horizontal acceleration. Nevertheless, they disregard the generation of parasitic vertical motion and seriously underestimate the distance to the free field. In closure, the criteria of significance of topography effects that the codes prescribe yield rational lower bounds for slope height H and inclination i, but do not take into account the effects of soil and excitation conditions. In remedy of these shortcomings, this paper proposed a set of tentative code provisions for topographic aggravation of seismic ground motion due to slope topography, as a basis of discussion.

9. REFERENCES

Ashford, S., Sitar, N., (1997), Analysis of topographic amplification of inclined shear waves in a steep coastal bluff, *Bulletin of the Seismological Society of America*, 87, no. 3, 692-700

Ashford, S., Sitar, N., Lysmer, J., Deng, N., (1997), Topographic effects on the seismic response of steep slopes, *Bulletin of the Seismological Society of America*, 87, no. 3, 701-709

Assimaki, D., Gazetas, G., (2004), Soil and topographic amplification on canyon banks and the Athens 1999 earthquake, *Journal of Earthquake Engineering*, 8, no. 1, 1-44

Athanasopoulos, G.A., Pelekis P.C., Xenaki V.C., (2001), Topography effects in the Athens 1999 earthquake: the case of hotel Dekelia, *Proceedings, 4th International Conference on Recent Advances in Geotechnical Earthquake Engineering and Soil Dynamics*, San Diego, March, (in CD-ROM)

Boore, D.M., Harmsen S.C., Harding, S.T., (1981), Wave scattering from a step change in surface topography, *Bulletin of the Seismological Society of America*, 71, no. 1, 117-125

Bouckovalas, G.D., Gazetas, G., Papadimitriou, A.G., (1999), Geotechnical aspects of the Aegion (Greece) earthquake, *Proceedings, 2nd International Conference on Geotechnical Earthquake Engineering*, Lisbon, June, vol. 2, 739-748

Bouckovalas, G.D., Papadimitriou, A.G. (2005), Numerical evaluation of slope topography effects on seismic ground motion, *Soil Dynamics and Earthquake Engineering*, 25, no. 7-10, 547-558

Gazetas, G., Kallou, P.V., Psarropoulos, P.N., (2002), Topography and soil effects in the Ms=5.9 Parnitha Athens earthquake: the case of Adames, *Natural Hazards*, 27, 133-169

Itasca Consulting Group Inc. (1992), FLAC: Fast Lagrangian Analysis of Continua. *User's Manual*.

Ohtsuki, A., Harumi, K., (1983), Effect of topography and subsurface inhomogeneities on seismic SV waves, *Earthquake Engineering and Structural Dynamics*, 11, 441-462